Available online at www.sciencedirect.com
ScienceDirect
Deep-Sea Research II 53 (2006) 2384–2397
DEEP-SEA RESEARCH PART II
www.elsevier.com/locate/dsr2

The effect of mesoscale iron enrichment on the marine photochemistry of dimethylsulfide in the NE subarctic Pacific

René-Christian Bouillon[a,*,1], William L. Miller[a,2], Maurice Levasseur[b,c], Michael Scarratt[b], Anissa Merzouk[c], Sonia Michaud[b], Lori Ziolkowski[a]

[a]*Department of Oceanography, Dalhousie University, Halifax, NS, Canada B3H 4J1*
[b]*Maurice Lamontagne Institute, Fisheries and Oceans Canada, 850, Route de la Mer, Mont-Joli, Que.,Canada G5H 3Z4*
[c]*Département de biologie, Univesité Laval, Québec-Océan, Sainte-Foy, Que., Canada G1K 7P4*

Received 16 September 2004; accepted 2 May 2006
Available online 29 September 2006

Abstract

Measurements of underwater light fields and available quantum yield spectra were used to calculate photochemical removal rates of DMS for surface waters of the northeast subarctic Pacific during the SERIES mesoscale iron-fertilization experiment in July 2002. We observed that the UV portion of the solar spectrum was most important in inducing DMS photo-oxidation, and calculated that UV-B accounted for more than 20% and UV-A for more than 68% of the total DMS photo-oxidation near the sea surface. Vertically resolved rates showed that most (>90%) of the DMS photo-oxidation occurs in the upper 15 m of the water column. During the study, calculated rates of DMS photo-oxidation, just below the ocean's surface ranged from 0.34 to 5.9 $\mu mol\, m^{-3}\, d^{-1}$. As the study progressed, an initial increase in photo-oxidation rates occurred within the iron-enriched patch and this was followed by a dramatic decrease in rates, whereas little change was observed outside the patch. Changes in DMS concentrations and decreases in the photochemical removal efficiency for DMS were the dominant factors explaining the variation in the DMS photo-oxidation rates. The turnover rate constants for DMS photo-oxidation, calculated for the upper mixed layer (UML) of the water column, ($0.03–0.25\, d^{-1}$) were in the range of those previously published and were at times higher than those calculated for biological consumption of DMS during SERIES. Our results suggest that iron fertilization of an oceanic patch in the northeast Pacific Ocean considerably altered the photochemical removal rates and turnover rate constants of DMS.

Keywords: Biogeochemical cycle; Photochemistry; Sulfur compounds; Dimethylsulfide; Iron; SERIES

1. Introduction

It has been proposed that factors controlling dimethylsulfide (DMS) concentrations in surface oceans indirectly affect atmospheric chemistry and potentially global climate (Charlson et al., 1987; Liss et al., 1997). DMS is the most abundant volatile reduced sulfur compound in well-oxygenated marine

*Corresponding author. Tel./fax: +1 416 978 3596.
E-mail address: rbouillo@chem.utoronto.ca (R.-C. Bouillon).
[1]Current address: Department of Chemistry, University of Toronto, Toronto, ON, Canada, M5S 3H6.
[2]Current address: Department of Marine Science, University of Georgia, Marine Sciences Bldg., Athens, GA 30602, USA.

0967-0645/$ - see front matter © 2006 Elsevier Ltd. All rights reserved.
doi:10.1016/j.dsr2.2006.05.024

surface waters. Marine emissions of DMS represent about 90% of the total sea-to-air transfer of reduced sulfur and may account for half of the global budget for biogenic sulfur entering the troposphere (Andreae, 1990; Malin et al., 1992). Atmospheric oxidation of DMS predominantly yields sulfates and aerosol particles that scatter and reflect incoming solar radiation. These aerosols also can act as cloud condensation nuclei (CCN), which influence cloud formation and thereby global climate (Charlson et al., 1987). DMS biogeochemistry is partially controlled by incident solar radiation reaching the surface ocean (Slezak et al., 2001; Toole et al., 2003). At present, the mechanisms responsible for DMS cycling are only poorly understood.

In oceanic waters, DMS cycling is a complex function of a number of biotic and abiotic processes (Liss et al., 1997). DMS is produced via the enzymatic cleavage of the algal osmolyte dimethylsulfoniopropionate (DMSP), the latter being synthesized by certain species of marine phytoplankton (Keller et al., 1989). Removal of DMS from surface oceans is known to occur as a result of three processes: sea–air transfer, photochemical oxidation, and bacterial consumption (Kieber et al., 1996; Liss et al., 1997). Since the sea-to-air flux of DMS is a function of the surface seawater concentration of DMS, it is essential to quantify the processes controlling the cycling of this compound in surface seawater.

Brimblecombe and Shooter (1986) first suggested that photochemical oxidation reactions might provide an important sink for DMS in the surface ocean. They found that the rate of the DMS photo-oxidation was directly proportional to the concentration of DMS and thus the reaction kinetics were pseudo first order. Since DMS does not absorb solar radiation in the wavelength range that reaches the ocean, DMS photo-oxidation must occur via an indirect photochemical pathway (Brimblecombe and Shooter, 1986). In addition to DMS concentration, the photo-oxidation rate of DMS in the surface ocean is controlled by several other environmental parameters (Brimblecombe and Shooter, 1986; Kieber et al., 1996; Brugger et al., 1998; Toole et al., 2003). As is the case for most environmental photochemical reactions, DMS photo-oxidation depends on the intensity and the spectral composition of solar radiation penetrating into the water column (Kieber et al., 1996). The quantity and quality of the incident irradiance are, in turn, controlled by the seawater optical properties (Kirk, 1994), which mainly depend on the abundance and composition of dissolved and suspended particulate organic and inorganic matter. In particular, absorption by chromophoric dissolved organic matter (CDOM) is thought to be responsible for most attenuation in the wavelength range (300–350 nm) relevant to DMS photochemistry (Johannsessen et al., 2003; Toole et al., 2003). This absorption generates reactive species or photo-oxidants that react with DMS (Kieber et al., 1996; Toole et al., 2003). In addition, it has been recently proposed that NO_3^- photolysis in seawater generates photo-oxidants such as $Br_2^{-\bullet}$, and $CO_3^{-\bullet}$ that readily oxidize DMS (Bouillon and Miller, 2004, 2005; Toole et al., 2004).

Some parts of the ocean are characterized by high-nitrate and low-chlorophyll concentrations (HNLC). These high-NO_3^- conditions have been attributed to low levels of iron that prevent phytoplankton growth and subsequent depletion of NO_3^- in the mixed layer (Martin and Fitzwater, 1988). The hypothesis of Martin and Fitzwater (1988) that phytoplankton productivity in these areas is limited by the availability of iron has being tested by performing several mesoscale iron addition experiments in the equatorial Pacific (Martin et al., 1994; Coale et al., 1996), the Southern Ocean (Boyd et al., 2000; Smetacek, 2001), and the North Pacific Ocean (Tsuda et al., 2003; Boyd et al., 2004). Results from these studies have clearly shown that addition of iron can significantly stimulate phytoplankton blooms. Studies that determined the concentration of biogenic sulfur compounds reported a considerable increase in DMS and DMSP concentrations over the measured period of the bloom in the equatorial Pacific (Turner et al., 1996) and in the Southern Ocean (Boyd et al., 2000).

Bouillon and Miller (2004) recently presented the temporal variation of the removal efficiency or apparent quantum yield for DMS photo-oxidation during the Subarctic Ecosystem Response to Iron Enhancement Study (SERIES). Le Clainche et al. (2006) have recently investigated the contributing physical, photochemical and biological processes to the DMS pool during SERIES using a DMS budget module embedded in a 1-D turbulent ocean model. In this study, we examined the effects of iron addition to an oceanic patch on the photo-oxidation and turnover rates of DMS. The wavelength- and depth-dependence of the DMS photo-oxidation rates and the evolution of the DMS photo-oxidation and turnover rates obtained during SERIES are

presented. We also evaluated the relative importance of different environmental factors in controlling the rates of DMS photo-oxidation. Furthermore the relative importance of photochemical processes as a sink for DMS were compared to biological consumption and atmospheric ventilation.

2. Methods

2.1. Study area and sampling

SERIES took place in July 2002, near Ocean Station Papa (50°N, 145°W) in the northeastern subarctic Pacific Ocean. The northeastern subarctic Pacific is recognized as one of the HNLC regions of the oceans where NO_3^- is generally not depleted at the surface (Harrison et al., 1999). On 9 July 2002, a 77 km^2 patch of ocean was fertilized with iron and tracked using sulfur hexafluoride (SF_6) (Law et al., 1998). A second infusion was performed on 16 July 2002. Additional information on the experimental design can be found in Boyd et al. (2004).

The iron-enriched patch (referred to here as "in-patch") and a reference station located northeast of the patch (referred to as "out-patch") were sampled from 10 to 28 July 2002 from the B.O. *El Puma*. Seawater was collected using either Niskin bottles secured to a rosette sampler or Go-Flo bottles. A CTD mounted in the center of the rosette was used to obtain vertical profiles for related oceanographic data during the descent.

2.2. Sample preparations and analysis

Photochemical experiments and the determination of seawater absorbance were performed in a shore-based laboratory using stored samples. At sea, water was gravity-filtered directly from a Go-Flo bottle through seawater-rinsed Whatman® POLYCAP AS 0.2 μm (820 cm^2) filter capsules into Nalgene® polycarbonate 2-L bottles. Prior to sample collection, filter capsules were extensively pre-cleaned with HCl solution and then with NANOpure-UV water. Samples were stored at 4 °C (dark) until used in irradiation experiments (about 5 months). It has been determined that sample storage did not considerably influence results (Bouillon, 2004). Just before each experiment, samples were re-filtered through a 0.2-μm Nylon membrane (Whatman®). The equipment and experimental procedures, for the determination of the pseudo first-order apparent quantum yield for DMS photo-oxidation ($AQY^*_{DMS}(\lambda)$) are given in Bouillon and Miller (2004). Absorbance spectra were measured in 10-cm quartz cells with a Varian CARY3 spectrophotometer and baseline corrected by subtracting the average apparent absorption from 600 to 700 nm from each spectrum. Absorption coefficients $a(\lambda)$ were calculated as: $a(\lambda) = 2.303A(\lambda)/l$, where $A(\lambda)$ is the measured absorbance at wavelength λ, and l is the path length (m) of the quartz cell.

2.3. Irradiance measurements

Vertical profiles of downwelling irradiance ($E_d(\lambda, z)$: mol photons $m^{-2}\,s^{-1}\,nm^{-1}$) throughout the photic layer were obtained with a SeaWiFS profiling multichannel radiometer (SPMR; Satlantic, Inc.), which measures radiation in thirteen wavebands, including four in the UV (2 nm bandwidth for 305, 323, 338, and 380 nm and 10 nm bandwidth for 412, 443, 490, 510, 532, 555, 670, 683, and 700 nm). An ocean color radiometer (OCR; Satlantic, Inc.) simultaneously measured incident downwelling irradiance just above the ocean's surface ($E_d(\lambda, 0+)$: mol photons $m^{-2}\,s^{-1}\,nm^{-1}$) in the same 13 wavebands as the profiler with an additional sensor at 590 nm. The OCR provided a wavelength matched surface reference for the profiler's irradiance measurements, correcting for changes in the incident irradiance during the profile.

Spectral attenuation coefficients ($K_d(\lambda)$: m^{-1}) were calculated from Eq. (1) for each profile over the first optical depth (from the surface to the depth at which the downwelling irradiance falls to $1/e$ of its surface value) using the Matlab® routine "ksurf". This in-house program (developed by R.F. Davis and modified by C. Fichot) makes use of the following relationship (Kirk, 1994):

$$K_d(\lambda) = \ln(E_d(\lambda, 0-)/E_d(\lambda, z + \Delta z))/\Delta z, \quad (1)$$

where $E_d(\lambda, 0-)$ (mol photons $m^{-2}\,s^{-1}\,nm^{-1}$) is the downwelling irradiance just below the ocean's surface and $E_d(\lambda, z + \Delta z)$ (mol photons $m^{-2}\,s^{-1}\,nm^{-1}$) is the downwelling irradiance at depth, both measured with the SPMR profiler and Δz is the change in depth, z (m). $K_d(\lambda)$ values for the unmeasured wavelengths were approximated by linear interpolation and extrapolation of the measured values. On board the ship, incident solar radiation was measured (60 Hz) using a multichannel visible detector system radiometer (MVDS: Satlantic, Inc.) mounted near the top of the mast of the B.O. *El Puma* with an unobstructed

view of the sky. Incident downwelling irradiance was recorded at seven wavelengths (325, 411, 442, 489, 554, 682, 699 nm) every 10 s and averaged hourly. Irradiance data from the MVDS were then used to scale a full spectrum solar irradiance model (Star solar model). The Star solar model (Ruggaber et al., 1994) was used to simulate the solar spectral irradiance reaching the water surface ($E_d(\lambda, 0+)$) as a function of latitude, time, total ozone, and other atmospheric parameters (Table 1). The downwelling spectral irradiance just below the sea-surface (($E_d(\lambda, 0-)$; mol photons $m^{-2} d^{-1} nm^{-1}$) was computed using the values of percentage irradiance loss by reflection at the sea–air interface (Whitehead et al., 2000) as a function of solar elevation (Jerlov, 1976) and wind speed (Austin, 1974).

$E_d(\lambda, 0-)$ was converted to downwelling scalar irradiance $E_o(\lambda, 0-)$, assuming that upwelling irradiance was negligible, using the relation

$$E_o(\lambda, 0-) \approx E_d(\lambda, 0-)/\bar{\mu}_d, \quad (2)$$

where $\bar{\mu}_d$ (dimensionless) is the average cosine of the downwelling irradiance. A fixed value of 0.86 for $\bar{\mu}_d$ was used in this study.

The modeled surface downwelling irradiance was then propagated through the water column using the measured spectral attenuation coefficients for downwelling irradiance ($K_d(\lambda)$: m^{-1}). The spectral downwelling irradiance $E_o(\lambda, 0-)$ at each depth (1 m interval), for wavelengths at 1-nm intervals ranging from 280 to 550 nm, was calculated using Beer's Law:

$$E_o(\lambda, z) = E_o(\lambda, 0-)e^{-K_d(\lambda)z}. \quad (3)$$

Table 1
Inputs (parameters) used to simulate the solar spectral irradiance reaching the sea surface with the Star solar model

Parameter description
Detector geometry: global irradiance
Wavelength field: UV-1 nm wvl
Output quantities: spectral
O_3: summer profile, 330 DU (TOMS: http://toms.gsfc.nasa.gov/ozone/ozone.html for 15 July 2002)
SO_2: not included
NO_2: not included
Pressure at ground: 1018.0 hPa
Temperature profile: summer.tem
Rel. humidity profile: summer.hum
Clouds: overcast conditions; base above ground 1.0 km; top above ground 1.4 km
Boundary layer depth: 3.0 km
Aerosol type: maritime clean air
Aerosol optical depth at 550 nm: 0.10
Stratospheric condition: background

2.4. Calculations

The wavelength dependence for the DMS photo-oxidation rates (mol DMS $m^{-3} d^{-1} nm^{-1}$) in surface waters was calculated using the expression below

$$-\frac{d[DMS]}{dt} = [DMS](E_o(\lambda, 0-))(a(\lambda))(AQY^*_{DMS}(\lambda)), \quad (4)$$

where [DMS] is the in situ DMS concentration in surface water (mol DMS m^{-3}) and $AQY^*_{DMS}(\lambda)$ represents the pseudo first-order apparent quantum yield for DMS photo-oxidation ((s^{-1})(mol photons absorbed $m^{-3} s^{-1}$)$^{-1}$) at a particular wavelength as determined and published in Bouillon and Miller (2004). It should be pointed out here that rate values have been corrected for the effect of temperature on DMS photo-oxidation rates in the ocean using the algorithms presented by Toole et al. (2003). A detailed examination of the DMS distribution during SERIES is presented elsewhere (Levasseur et al., this issue). In situ DMS concentrations were not measured on 12 July out-patch. In order to calculate photo-oxidation rates of DMS for the 12 July out-patch station, we used instead in situ DMS concentrations measured on 10 July out-patch.

The DMS photo-oxidation rates (mol DMS $m^{-3} d^{-1}$), integrated for irradiation over the wavelength range 280–550 nm, as a function of depth were computed using Eq. (5):

$$-\frac{d[DMS]}{dt} = [DMS]\int_{\lambda=280}^{550}(E_o(\lambda, z)) \times (a(\lambda))(AQY^*_{DMS}(\lambda))\, d\lambda. \quad (5)$$

The vertical distribution of DMS was not uniform throughout the upper 20 m of the water column during SERIES (Levasseur et al., this issue). For this study, DMS concentrations were calculated at increments of 1 m down to 20 m depth by interpolating the in situ concentrations. $AQY^*_{DMS}(\lambda)$ and $a(\lambda)$ were assumed to be constant over the depth interval considered (0–20 m).

In order to evaluate the relative importance of photochemical processes as a removal mechanism for DMS during SERIES, turnover rate constants (k_τ) for DMS photo-oxidation were calculated for

the upper mixed layer (UML). Calculations were achieved by dividing total DMS present in the UML of the water column ($[DMS]_{0-MLD}$: mol DMS m^{-2}) by the daily depth-integrated (from 0 m to the mixed-layer depth (MLD)) DMS photochemical loss, (Rate UML: mol DMS $m^{-2} d^{-1}$). Rate UML was calculated using the following equation:

$$\text{Rate UML} = \int_{\lambda=280}^{550} \int_{z=0}^{\text{MLD}} [\text{DMS}](E_o(\lambda, z))(a(\lambda)) \times (\text{AQY}^*_{\text{DMS}}(\lambda))\, d\lambda\, dz. \quad (6)$$

The turnover rate constant k_τ (d^{-1}) for DMS photo-degradation is

$$k_\tau = \text{Rate UML}/[\text{DMS}]_{0-\text{MLD}}. \quad (7)$$

Estimation of the emission rate of DMS from sea to atmosphere (Flux: mol $m^{-2} d^{-1}$) is expressed as (Liss, 1973; Kettle and Andreae, 2000)

$$\text{Flux} = k_{t-\text{DMS}} [\text{DMS}]_w, \quad (8)$$

where k_{t-DMS} is the sea–air gas transfer velocity coefficient for DMS (m d^{-1}) and $[DMS]_w$ represents DMS concentrations in water (mol m^{-3}). k_{t-DMS} was calculated with the relationship proposed by Liss and Merlivat (1986) using the surface seawater temperature and local wind speeds measured at a height of 10 m above the water surface (Phinney et al., this issue). The daily turnover rate constant for atmospheric ventilation was calculated by dividing the sea–air flux by the depth-integrated DMS concentration over the UML of the water column.

Bacterial consumption rates of DMS were determined at one depth (~10 m). The methods used to determine the bacterial consumption and a detailed examination of these results are presented elsewhere in this issue (Merzouk et al., this issue). The daily turnover rate constant for bacterial consumption was calculated by dividing the bacterial consumption rates by the averaged DMS concentration in the UML of the water column. For sake of comparison with other loss processes, we assumed that the rates of bacterial consumption of DMS are constant in the UML of the water column. It should be mentioned that the bacterial consumption rates of DMS was not determined on 12 July out-patch. DMS turnover rate constant for biological consumption referred to as "12 July out-patch" was actually determined on 10 July out-patch.

3. Results and discussion

Evidence has been recently reported for a significant chemical and biological response within the upper water column upon addition of iron during SERIES (Boyd et al., 2004). Boyd and coworkers observed that iron fertilization triggered a large increase in chlorophyll concentrations (~6 × background) and a drawdown of silicates and NO_3^- by phytoplankton. The mesoscale iron addition also resulted in significant changes in DMS and DMSP concentrations (Levasseur et al., this issue) and DMS atmospheric ventilation fluxes. The average DMS concentration in the UML of the water column ranged from 1.4 to 17.2 μmol m^{-3} (Fig. 1A). The temporal evolution of DMS concentrations inside the patch consisted of an initial increase followed by a 12-fold decrease that was likely caused by a shift in phytoplankton community structure and DMSP bacterial metabolism (Levasseur et al., this issue; Merzouk et al., this issue). The iron addition initially caused a bloom of haptophytes, a phytoplankton group known to produce copious amount of DMSP, the precursor of DMS (Keller et al., 1989). After about 1 week, the abundance of haptophytes declined considerably apparently due to intense micro-zooplankton grazing (Levasseur et al., this issue). This period coincided with low or negative net DMS production rates suggesting that most of the DMSP released was demethylated (Merzouk et al., this issue). The iron addition also stimulated a massive diatom bloom that became dominant over the initial phytoplankton community about 10 days after the initial iron addition. Diatoms are a phytoplankton group known as poor DMS and DMSP producers (Keller et al., 1989).

This study presents the photochemical oxidation rates of DMS calculated during SERIES. The calculation of these rates required information on in situ DMS concentration (Levasseur et al., this issue), seawater absorption coefficient (Fig. 1B), seawater temperature (Fig. 1C), seawater attenuation coefficient (Fig. 2), downwelling solar irradiance (Fig. 3), and the apparent quantum yield for DMS photo-oxidation (Bouillon and Miller, 2004). These factors are presented in this work to help the readers in the interpretation of the results. However, the spatial and temporal variability of these factors will not be discussed in detail here.

The wavelength-dependence for DMS photo-oxidation rates in SERIES surface water was

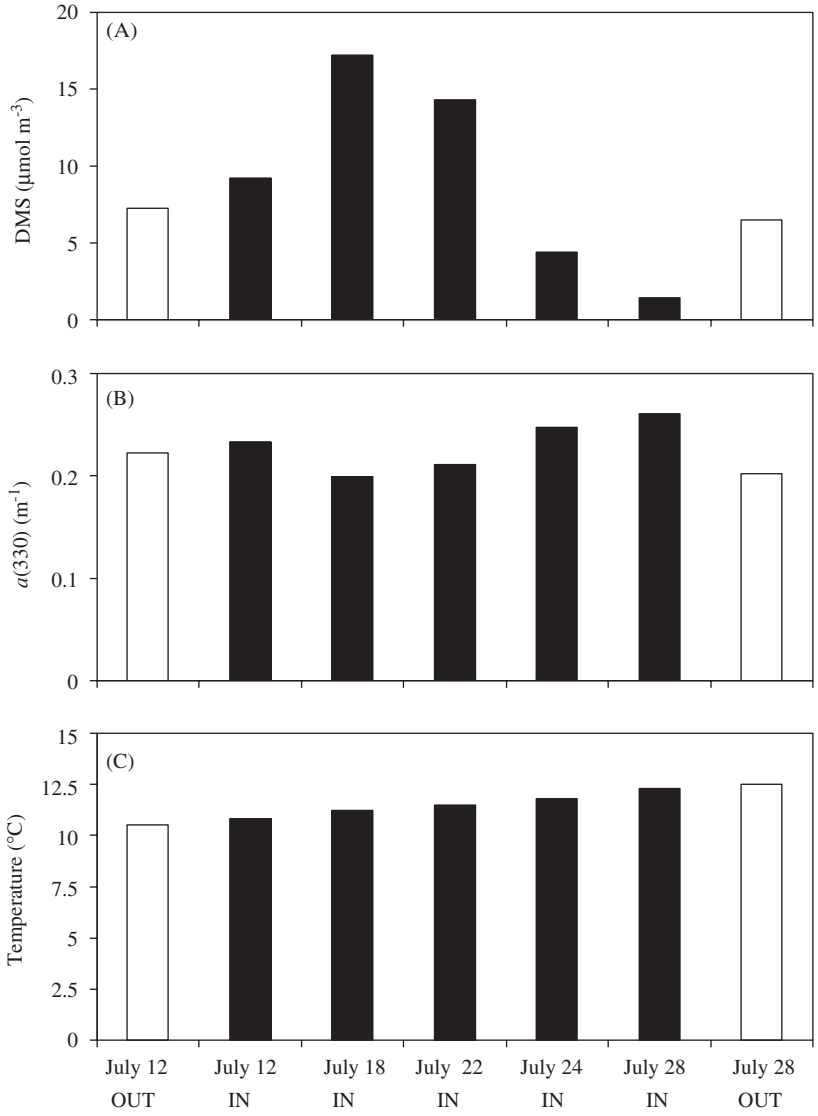

Fig. 1. Average DMS concentrations in the upper mixed layer (A), surface seawater absorption coefficient determined at 330 nm (a(330)) (B), and surface seawater temperature (C) measured during the SERIES project in July 2002 (white bars: out-patch; black bars: in-patch).

calculated using Eq. (4) for samples collected on 12 and 28 July inside and outside the patch (Fig. 4). The results clearly demonstrate that DMS photo-oxidation is initiated mainly by UV solar radiation, primarily at wavelengths between 310 and 360 nm, with visible light having little effect. Maximum photo-oxidation was observed at 326 and 330 nm on 12 and 28 July, respectively. This is similar to what Toole et al. (2003) observed in the Sargasso Sea. In contrast, Kieber et al. (1996) found that, in samples collected from the equatorial Pacific, the photo-oxidation of DMS occurred principally in the 380–460-nm wavelength range with minimal photo-chemical degradation generated by the UV-B (280–320 nm) and UV-A (320–400 nm) wavelengths. It should be pointed out that the Kieber et al. (1996) observations are somewhat uncommon in the field of environmental aquatic photochemistry. Indeed, it has been generally observed that UV-A and UV-B radiation are most important at initiating the photochemical production for a variety of products such as CO (Miller et al., 2002), COS (Zepp and Andreae, 1994), CS_2 (Xie et al., 1998), H_2O_2 (Yocis et al., 2000), and $OH^{\bullet}$ radicals (Qian et al., 2001). In this study, we calculated that UV-B accounted for more than 20% and UV-A for more than 68% of

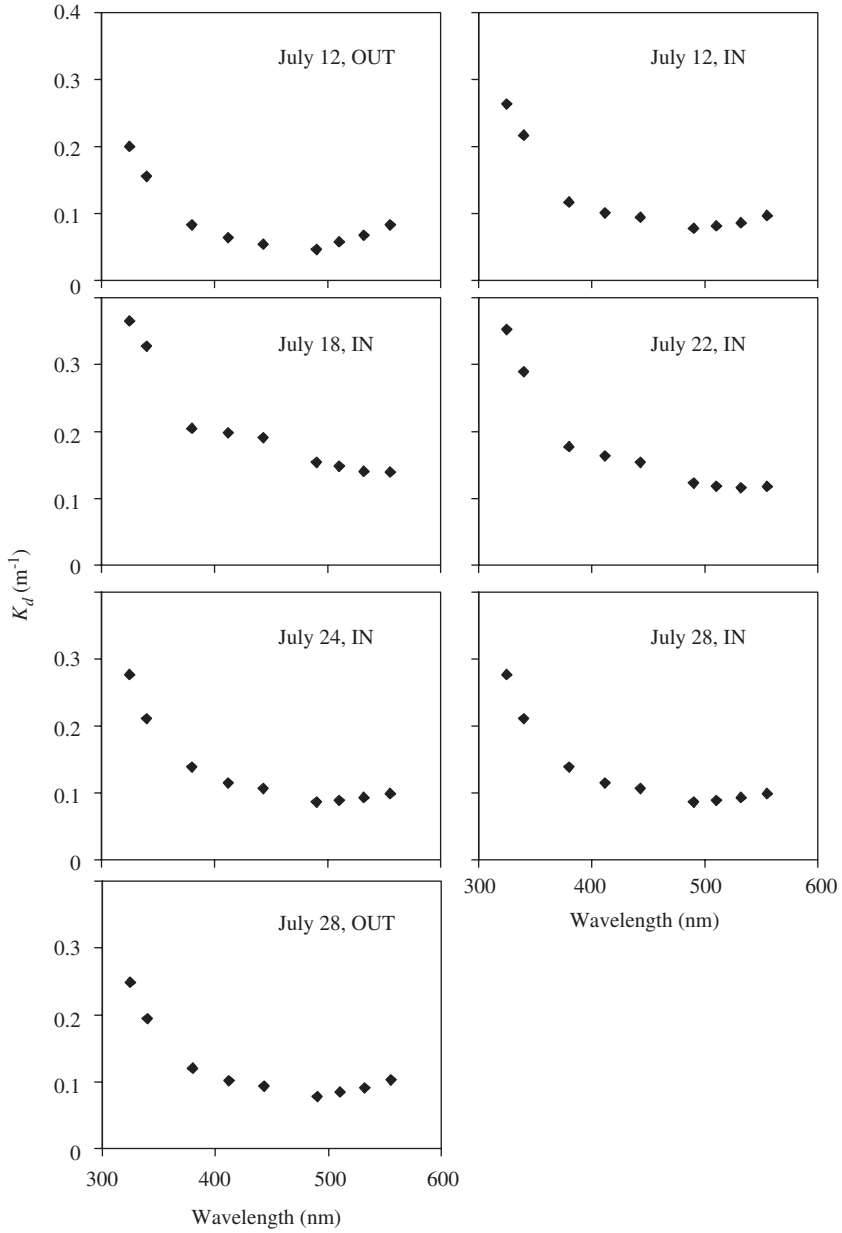

Fig. 2. Measured downwelling attenuation coefficient ($K_d(\lambda)$) during the SERIES project in July 2002.

the total DMS photo-oxidation near the sea surface (Table 2). These results are again consistent with Toole et al. (2003) who calculated that, in surface Sargasso Sea waters, UV-B and UV-A radiation contributed about 32.6% and 67.4% of the DMS photo-oxidation loss, respectively. One striking observation from Fig. 4 is that while both 12 July in-patch and out-patch samples showed approximately the same magnitude in rates, the rates calculated for the 28 July in-patch sample are considerably lower than for the out-patch sample collected on the same day. Temporal variations in DMS photo-oxidation rates will be discussed in detail below.

Photo-oxidation rates for DMS were calculated as a function of depth in the water column based on in situ DMS concentrations and solar irradiance data from the Star model (Eq. (5)). Higher DMS photo-oxidation rates were always observed near the surface where solar irradiance is highest and

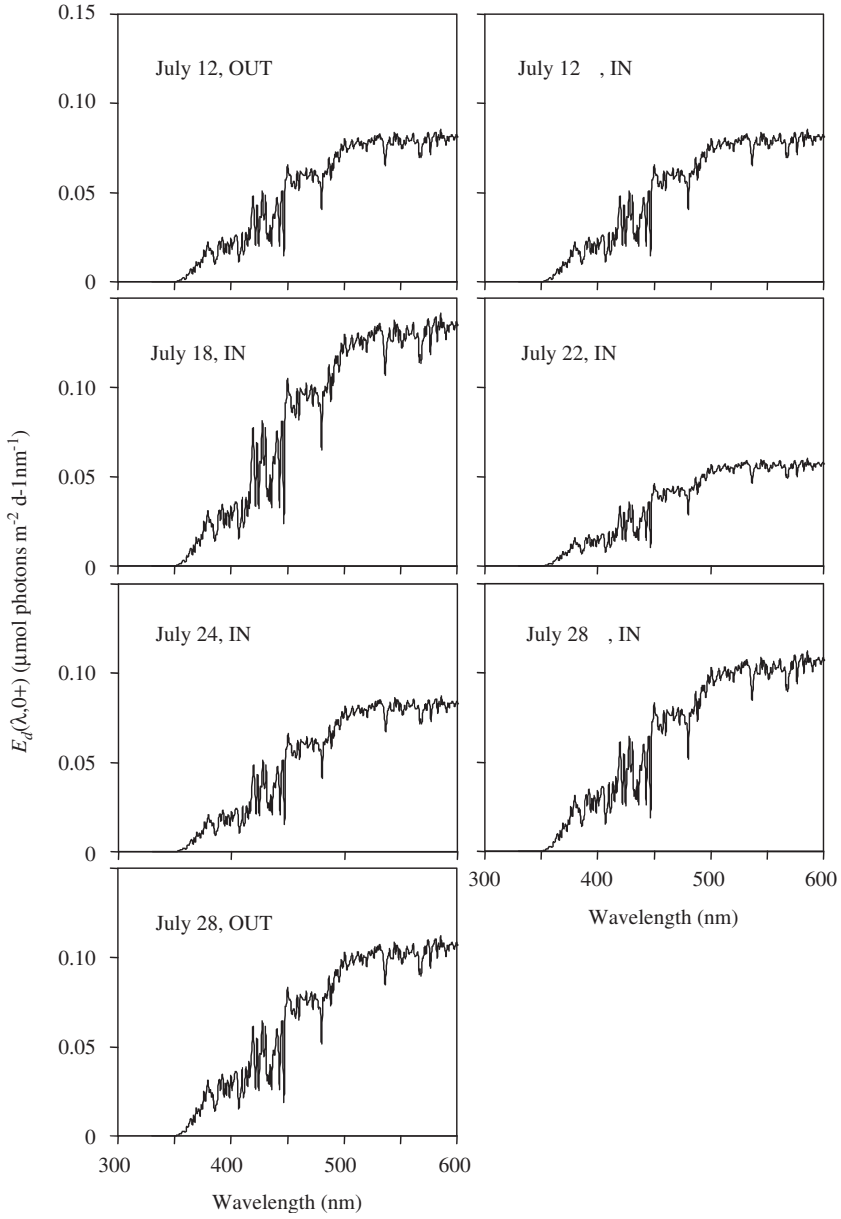

Fig. 3. Modeled surface downwelling spectral irradiance reaching the water surface ($E_d(\lambda, 0+)$), using the Star solar model, during the SERIES project in July 2002.

rates decrease rapidly with depth (Fig. 5). DMS photo-oxidation was limited to the upper few meters of both fertilized and unfertilized water column in the northeast Pacific waters as shown in Fig. 5. Vertical integration show that more than 90% of the photo-oxidation occurred in the top 15 m even in the samples with the lowest optical attenuation. This is in contrast to the results from Kieber et al. (1996) that indicated that DMS photo-oxidation was still significant at depths greater than 50 m in the equatorial Pacific. This discrepancy between results from Kieber et al. (1996) and our results derives from the difference in seawater optical properties and from wavelength-dependency of DMS photo-oxidation observed in both studies.

Calculated DMS photo-oxidation rates just below the ocean's surface (Rate (0 m)) during SERIES ranged from 0.34 to 5.9 µmol m^{-3} d^{-1} (Fig. 6A). From 12 to 18 July, we observed an initial increase in calculated DMS photo-oxidation rates within the

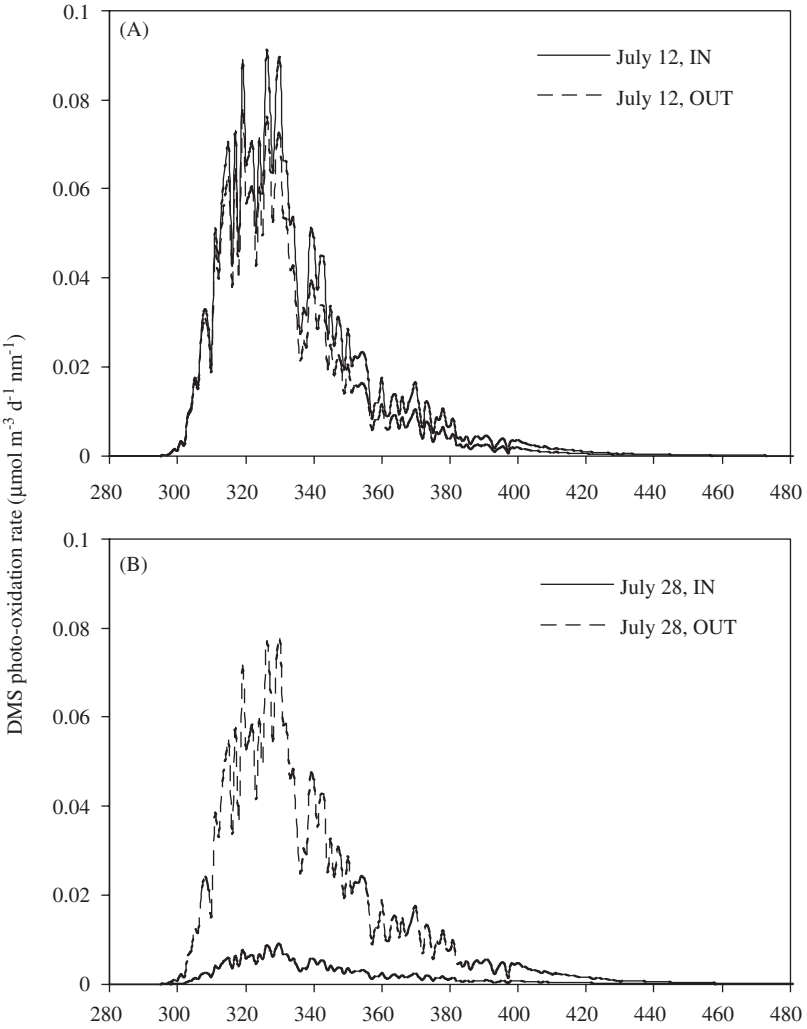

Fig. 4. DMS photo-oxidation rate just below the surface plotted as a function of wavelength calculated for 12 July 2002 (A) and 28 July 2002 (B) at in-patch and out-patch stations.

Table 2
Calculated spectral partitioning of UV-B (280–320 nm) and UV-A (320–400 nm) radiation contribution to the total DMS photo-oxidation calculated for 12 and 28 July 2002 at in-patch and out-patch stations during SERIES

Station	UV-B (%)	UV-A (%)
12 July IN	27.1	71.0
12 July OUT	30.6	68.3
28 July IN	20.6	74.7
28 July OUT	23.2	73.6

patch followed by a ~17-fold decrease from 18 to 28 July. On the other hand, at the out-patch station a minor increase was noticed from 12 to 28 July. The temporal variability of Rate (0 m) calculated in this study could be attributed to the variation of any or all of the following factors: DMS concentration, seawater absorption coefficient (a proxy for CDOM concentration) ($a(\lambda)$), UV radiation intensity ($E_o(\lambda, z)$), the photochemical removal efficiency for DMS ($AQY^*_{DMS}(\lambda)$) and seawater temperature.

The relative contribution of each of these factors to the temporal variability of Rate (0 m) for each station has been calculated relative to out-patch values of 12 July (Table 3). For example, by calculating Rate (0 m) (Eq. (5)) using values of $E_o(\lambda, z)$, $a(\lambda)$, $AQY^*_{DMS}(\lambda)$ and seawater temperature determined at the 12 July out-patch station and changing only the DMS concentrations to those calculated at the 18 July in-patch station, we could evaluate (for 18 July in-patch) the specific

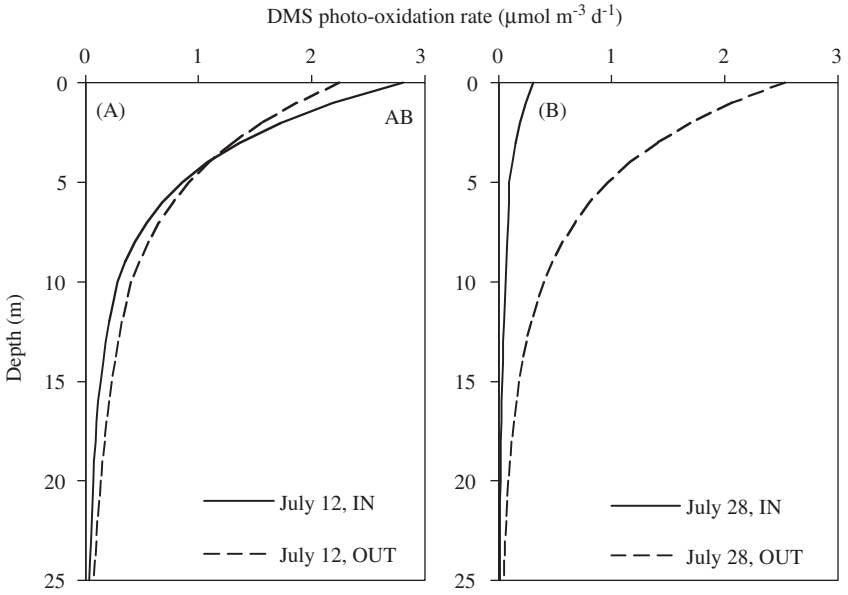

Fig. 5. DMS photo-oxidation rate plotted as a function of depth calculated for 12 July 2002 (A) and 28 July 2002 (B) at in-patch and out-patch stations.

contribution of the variation in DMS concentration to the variation in Rate (0 m). We calculated that the change in DMS concentration in the patch was the most important factor affecting the variation of Rate (0 m) between 12 July out-patch and 18 July in-patch (Table 3). The lowest Rate (0 m) value in this study was calculated on 28 July at the in-patch station and is mainly the result of the combination of a large decrease in both in situ DMS concentrations and $AQY^*_{DMS}(\lambda)$ values (Figs. 1A, 6B). On the other hand, only a 13% increase in Rate (0 m) values has been observed between 12 and 28 July at the out-patch station resulting from a small change in $AQY^*_{DMS}(\lambda)$ values and DMS concentrations. As discussed in Bouillon and Miller (2004), a significant decrease in the pseudo first-order spectral apparent quantum yield (represented by data from 330 nm: $AQY^*_{DMS}(330\,nm)$) was detected within the patch between 12 and 28 July (Fig. 6B). It has been suggested that this decrease in $AQY^*_{DMS}(330\,nm)$ was associated with a corresponding decrease in NO_3^- concentrations triggered by the iron addition (Bouillon and Miller, 2004; Boyd et al., 2004). This finding suggests that marine micro-organisms indirectly control DMS photo-oxidation rates by controlling both DMS concentrations and $AQY^*_{DMS}(330\,nm)$, the latter being partially controlled by NO_3^- concentrations (Bouillon and Miller, 2004).

In order to compare our results with those published elsewhere, we calculated the turnover rate constant (k_τ) for DMS photochemical removal in the UML (see Eqs. (5) and (6)). k_τ calculated during SERIES ranged from 0.03 to 0.25 d^{-1}. On 12 July, k_τ values were fairly similar at both in-patch and out-patch stations. However on 28 July, the k_τ value calculated at the out-patch station was about twice as high as the one calculated for the in-patch station, suggesting that iron fertilization had influenced the turnover rate of DMS. A comparison of turnover rate constants calculated in this study with other published studies is presented in Table 4. k_τ values for SERIES were in the same range as those obtained in the equatorial Pacific, North Sea, North Atlantic, Adriatic Sea and the Sargasso Sea (Kieber et al., 1996; Brugger et al., 1998; Simó and Pedrós-Alió, 1999; Hatton, 2002; Toole et al., 2003).

We also examined the importance of DMS photo-oxidation as a removal mechanism for DMS relative to biological consumption and atmospheric ventilation of DMS. During SERIES, the turnover rate constants in the UML of the water column ranged from 0.0 to 1.0 d^{-1} for the biological removal of DMS (Merzouk et al., this issue) and from 0.03 to 0.22 d^{-1} for atmospheric ventilation of DMS (Fig. 7). We calculated that photochemical reactions contributed from 6% to 55% of the total loss of DMS in the UML of the water column over the

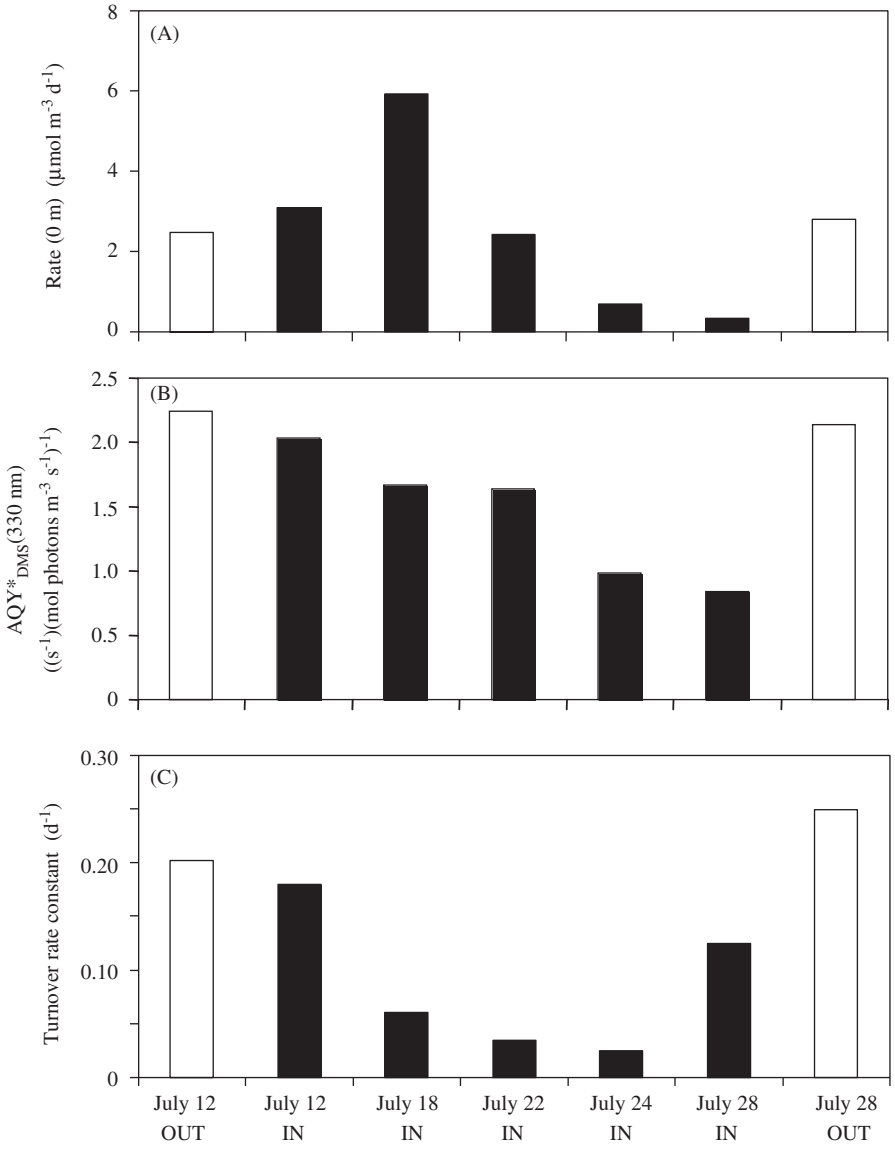

Fig. 6. DMS photo-oxidation rates just below the surface (Rate (0 m)) (A), pseudo first-order apparent quantum yield at 330 nm for DMS photo-oxidation (AQY^*_{DMS}(330 nm)) (from Bouillon and Miller, 2004) (B), and turnover rate constants for DMS photo-oxidation for the upper mixed layer of the water column (C) calculated during the SERIES project in the northeastern Pacific in July 2002 (white bars: out-patch; black bars: in-patch).

Table 3
The relative contribution of the different environmental factors to the temporal variability of Rate (0 m) for each station during SERIES in July 2002 calculated relative to values from 12 July out-patch

Station	DMS (%)	E_d (λ, z) (%)	$a(\lambda)$ (%)	AQY^*_{DMS} (λ) (%)	Temparature (%)
12 July IN	+29	0	+4	−7	+0.9
18 July IN	+139	+40	−10	−25	+2.2
22 July IN	+104	−31	−5	−27	+3.2
24 July IN	−39	−6	+11	−56	+4.2
28 July IN	−80	+38	+17	−59	+5.9
28 July OUT	−2	+52	+1	+13	+6.6

Table 4
Comparison of turnover rate constants calculated for this study (SERIES, northeast Pacific Ocean, July 2002) and other studies

Location	Turnover rate constant (d^{-1})	Depth interval (m)	Study
Northeast Pacific	0.03–0.25	UML[a]	This study
Equatorial Pacific	0.1–0.3	UML[a]	Kieber er al. (1996)
Coastal Adriatic Sea	0.32 ± 0.05	0–20 m	Brugger et al. (1998)
North Atlantic	0.1 ± 2.5	UML[a]	Simó and Pedrós-Alió (1999)
North Sea	0.1–0.37	0–20 m	Hatton (2002)
Sargasso Sea	0.01–0.22	UML[a]	Toole et al. (2003)

[a]UML: upper mixed layer.

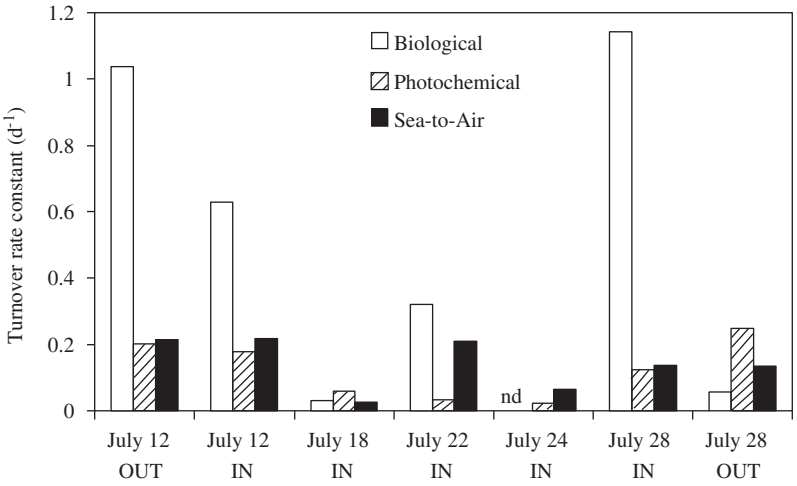

*nd: non-detected

Fig. 7. Comparison of the DMS turnover rate constants for biological, photochemical and sea–air ventilation processes during the SERIES project in the northeastern Pacific in July 2002 calculated for the upper mixed layer of the water column. It should be mentioned that the DMS turnover rate constant for biological consumption was not determined on 12 July out-patch. The value referred to here as "12 July out-patch" was actually determined on 10 July out-patch.

same period. A large variability in the relative importance of photo-oxidation as a removal process for DMS in the UML also has been observed by Kieber et al. (1996), who reported values ranging from 7% to 40% in the equatorial Pacific. It should be pointed out that DMS photo-oxidation was the dominant removal pathway for DMS on 18 July in-patch and 28 July out-patch.

4. Conclusion

Results from this study agree with previous work in that DMS photochemical removal in the northeastern Pacific Ocean during SERIES was found to be a significant sink for DMS, and on occasion the dominant removal pathway. Our results indicate that DMS photo-oxidation was mainly driven by solar radiation in the UV wavelength range, and consequently was limited to the upper ~15 m of the water column. Inside the iron-fertilized patch, the evolution of the photochemical DMS removal rates was mainly associated with variation of DMS and NO_3^- concentrations resulting from the iron-induced phytoplankton bloom. Our results suggest that iron fertilization of an oceanic patch in the northeast Pacific Ocean can considerably alter the photochemical removal rates of DMS.

Acknowledgments

The authors thank the officers and crew of the B.O. *El Puma*. We also thank Robert M. Moore for loan of analytical equipment. We are grateful to Lisa Phinney for making available unpublished

data. The constructive criticisms provided by two anonymous reviewers on an earlier version of this manuscript are gratefully acknowledged. This work was supported by Natural Sciences and Engineering Research Council (NSERC) of Canada, Canadian Foundation for Climate and Atmospheric Sciences (CFCAS), and National Science Foundation (NSF, OCE0326685). RCB was supported by post-graduate scholarships from Fonds pour la Formation de Chercheurs et l'Aide à la Recherche (Fonds FCAR) and NSERC of Canada.

References

Andreae, M.O., 1990. Ocean–atmosphere interactions in the global biogeochemical sulfur cycle. Marine Chemistry 30, 1–29.

Austin, R.W., 1974. The remote sensing of spectral radiance from below the ocean surface. In: Jerlov, N.G., Steemann Nielsen, E. (Eds.), Optical Aspects of Oceanography. Academic Press, London, UK, pp. 317–344.

Bouillon, R.-C., 2004. An investigation on the photochemistry of dimethylsulfide in marine waters. Ph.D. Thesis, Dalhousie University, Halifax, Canada, unpublished.

Bouillon, R.C., Miller, W.L., 2004. Determination of apparent quantum yield spectra of DMS photo-degradation in an in situ iron-induced Northeast Pacific Ocean bloom. Geophysical Research Letters 31, L06310.

Bouillon, R.C., Miller, W.L., 2005. Photodegradation of dimethyl sulfide (DMS) in naturals waters: laboratory assessment of the nitrate-induced DMS oxidation. Environmental Science and Technology 39 (24), 9471–9477.

Brimblecombe, P., Shooter, D., 1986. Photo-oxidation of dimethylsulphide in aqueous solution. Marine Chemistry 19 (4), 343–353.

Brugger, A., Slezak, D., Obernosterer, I., Herndl, G.J., 1998. Photolysis of dimethylsulfide in the northern Adriatic Sea: dependence on substrate concentration, irradiance and DOC concentration. Marine Chemistry 59 (304), 321–331.

Boyd, P.W., Watson, A.J., Law, C.S., Abraham, E.R., Trull, T., Murdoch, R., Bakker, D.C.E., Bowie, A.R., Buesseler, K.O., Chang, H., Charette, M., Croot, P., Downing, K., Frew, R., Gall, M., Hadfield, M., Hall, J., Harvey, M., Jameson, G., Laroche, J., Liddicoat, M., Ling, R., Maldonado, M.T., McKay, R.M., Nodder, S., Pickmere, S., Pridmore, R., Rintoul, S., Safi, K., Sutton, P., Strzepek, R., Tanneberger, K., Turner, S., Waite, A., Zeldis, J., 2000. A mesoscale phytoplankton bloom in the polar Southern Ocean stimulated by iron fertilization. Nature 407, 695–702.

Boyd, P.W., Law, C.S., Wong, C.S., Nojiri, Y., Tsuda, A., Levasseur, M., Takeda, S., Rivkin, R., Harrison, P.J., Strzepek, R., Gower, J., McKay, R.M., Abraham, E., Arychuk, M., Barwell-Clarke, J., Crawford, W., Crawford, D., Hale, M., Harada, K., Johnson, K., Kiyosawa, H., Kudo, I., Marchetti, A., Miller, W.L., Needoba, J., Nishioka, J., Ogawa, H., Page, J., Robert, M., Saito, H., Sastri, A., Sherry, N., Soutar, T., Sutherland, N., Taira, Y., Whitney, F., Wong, S.-K.E., Yoshimura, T., 2004. The decline and fate of an iron-induced subarctic phytoplankton bloom. Nature 428, 549–553.

Charlson, R.J., Lovelock, J.E., Andreae, M.O., Warren, S.G., 1987. Oceanic phytoplankton, atmospheric sulphur, cloud albedo and climate. Nature 326, 655–661.

Coale, K.H., Johnson, K.S., Fitzwater, S.E., Gordon, R.M., Tanner, S., Chavez, F.P., Ferioli, L., Sakamoto, C., Rogers, P., Millero, F., Steinberg, P., Nightingale, P., Cooper, D., Cochlan, W.P., Landry, M.R., Constantinou, J., Rollwagen, G., Trasvina, A., Kudela, P., 1996. A massive phytoplankton bloom induced by an ecosystem-scale iron fertilization experiment in the equatorial Pacific Ocean. Nature 383, 495–501.

Harrison, P.J., Boyd, P.W., Varela, D.E., Takeda, S., Shiomoto, A., Odate, T., 1999. Comparison of factors controlling phytoplankton productivity in the NE and NW Subarctic Pacific Gyres. Progress in Oceanography 43 (2–4), 205–234.

Hatton, A.D., 2002. Influence of photochemistry on the marine biogeochemical cycle of dimethylsuphide in the northern North Sea. Deep-Sea Research II 49 (15), 3039–3305.

Jerlov, N.G., 1976. Marine optics. Elsevier Scientific, New York.

Johannsessen, S.C., Miller, W.L., Cullen, J.J., 2003. Calculation of UV attenuation and colored dissolved organic matter absorption coefficient spectra from measurements of ocean color. Journal of Geophysical Research 108 (C9), 3301.

Keller, M.D., Bellows, W.K., Guillard, R.R.L., 1989. Dimethyl sulfide production in marine phytoplankton. In: Saltzman, E.S., Cooper, W.J. (Eds.), Biogenic Sulfur in the Environment. American Chemical Society, Washington, DC, pp. 167–182.

Kettle, A.J., Andreae, M.O., 2000. Flux of dimethylsulfide from the oceans: a comparison of updated data sets and flux models. Journal of Geophysical Research 105 (D22), 26793–26808.

Kieber, D.J., Jiao, J., Kiene, R.P., Bates, T.S., 1996. Impact of dimethylsulfide photochemistry on methyl sulfur cycling in the equatorial Pacific Ocean. Journal of Geophysical Research 101 (C2), 3715–3722.

Kirk, J.T.O., 1994. Light and Photosynthesis in Aquatic Systems, second ed. Cambridge University Press, Cambridge, UK.

Law, C.S., Watson, A.J., Liddicoat, M.I., Stanton, T., 1998. Sulphur hexafluoride as a tracer of biogeochemical and physical processes in an open-ocean iron fertilization experiments. Deep-Sea Research II 45 (6), 977–994.

Le Clainche, Y., Levasseur, M., Vézina, A., Bouillon, R.-C., Merzouk, A., Michaud, S., Scarratt, M., Wong, C.S., Rivkin, R.B., Boyd, P.W., Harrison, P.J., Miller, W.L., Law, C.L., Saucier, F.J., 2006. Modeling analysis of the effect of iron enrichment on DMS dynamic in the NE Pacific (SERIES experiment). Journal of Geophysical Research 111 (C1), C01011.

Levasseur, M., Scarratt, M.G., Michaud, S., Merzouk, A., Wong, C.S., Arychuk, M., Richardson, W., Wong, E., Marchetti, A., Kiyosawa, H. DMSP and DMS dynamics during a mesoscale iron fertilization experiment in the Northeast Pacific. Part I. Temporal and vertical distributions, Deep-Sea Research II, this issue [doi:10.1016/j.dsri2.2006.05.023].

Liss, P.S., 1973. Processes of gas exchange across an air–water interface. Deep-Sea Research 20 (3), 221–238.

Liss, P.S., Merlivat, L., 1986. Air–sea exchange rates: introduction and synthesis. In: Menard, P.B. (Ed.), The Role of

Air-Sea Exchange in Geochemical Cycling. D. Reidel Publishing Company, Berlin, pp. 113–127.

Liss, P.S., Hatton, A.D., Malin, G., Nightingale, P.D., Turner, S.M., 1997. Marine sulphur emissions. Philosophical Transactions of the Royal Society of London B: Biological Sciences 352 (1350), 159–169.

Malin, G., Turner, S.M., Liss, P.S., 1992. Sulfur: the plankton/climate connection. Journal of Phycology 28 (5), 590–597.

Martin, J.H., Fitzwater, S.E., 1988. Iron deficiency limits phytoplankton growth in northeast Pacific subarctic. Nature 331, 341–343.

Martin, J.H., Coale, K.H., Johnson, K.S., Fitzwater, S.E., Gordon, R.M., Tanner, S.J., Hunter, C.N., Elrod, V.A., Nowicki, J.L., Coley, T.L., Barber, R.T., Lindley, S., Watson, A.J., Van Scoy, K., Law, C.S., Liddicoat, M.I., Ling, R., Stanton, T., Stockel, J., Collins, C., Anderson, A., Bidigare, R., Ondrusek, M., Latasa, M., Millero, F.J., Lee, K., Yao, W., Zhang, J.Z., Friederich, G., Sakamoto, C., Chavez, F., Buck, K., Kolber, Z., Greene, R., Falkowski, P., Chisholm, S.W., Hoge, F., Swift, R., Yungel, J., Turner, S., Nightingale, P., Hatton, A., Liss, P., Tindale, N.W., 1994. Testing the iron hypothesis in ecosystems of the equatorial Pacific Ocean. Nature 371, 123–129.

Merzouk, A., Levasseur, M., Scarratt, M., Michaud, S., Rivkin, R., Hale, M., Kiene, R., Price, N. DMSP and DMS dynamics during a mesoscale iron fertilization experiment in the Northeast Pacific, Part II. Biological cycling. Deep-Sea Research II, this issue [doi:10.1016/j.dsr2.2006.05.022].

Miller, W.L., Moran, M.A., Sheldon, W.M., Zepp, R.G., Opsahl, S., 2002. Determinations of apparent quantum yield spectra for the formation of biologically labile photoproducts. Limnology and Oceanography 47 (2), 343–352.

Phinney, L., Leaitch, W.R., Lohmann, U., Boudries, H., Worsnop, D.R., Jayne, J.T., Toom-Sauntry, D., Wadleigh, M., Sharma, S., Shantz, N. Characterization of the aerosol over the Sub-arctic North East Pacific Ocean. Deep-Sea Research II, this issue [doi:10.1016/j.dsr2.2006.05.044].

Qian, J., Mopper, K., Kieber, D.J., 2001. Photochemical production of the hydroxyl radical in Antarctic waters. Deep-Sea Research I 48 (3), 741–759.

Ruggaber, A., Dlugi, R., Nakajima, T., 1994. Modelling of radiation quantities and photolysis frequencies in the troposphere. Journal of Atmospheric Chemistry 18 (2), 171–210.

Simó, R., Pedrós-Alió, C., 1999. Short-term variability in the open ocean cycle of dimethylsulfide. Global Biogeochemical Cycles 13 (4), 1173–1181.

Slezak, D., Brugger, A., Herndl, G.J., 2001. Impact of solar radiation on the biological removal of dimethylsulfoniopropionate and dimethylsulfide in marine surface waters. Aquatic Microbial Ecology 25 (1), 87–97.

Smetacek, V., 2001. EisenEx, International team conducts iron experiment in the Southern Ocean. US JGOFS New 11 (1), 11–14.

Toole, D.A., Kieber, D.J., Kiene, R.P., Siegel, D.A., Nelson, N.B., 2003. Photolysis and the dimethylsulfide (DMS) summer paradox in the Sargasso Sea. Limnology and Oceanography 48 (3), 1088–1100.

Toole, D.A., Kieber, D.J., Kiene, R.P., White, E.M., Bisgrove, J., del Valle, D.A., Slezak, D., 2004. High dimethylsulfide photolysis rates in nitrate-rich Antarctic waters. Geophysical Research Letters 31, L11307.

Tsuda, A., Takeda, S., Saito, H., Nishioka, J., Nojiri, Y., Kudo, I., Kiyosawa, H., Shiomoto, A., Imai, K., Ono, T., Shimamoto, A., Tsumune, D., Yoshimura, T., Aono, T., Hinuma, A., Kinugasa, M., Suzuki, K., Sohrin, Y., Noiri, Y., Tani, H., Deguchi, Y., Tsurushima, N., Ogawa, H., Fukami, K., Kuma, K., Saino, T., 2003. A mesoscale iron enrichment in the western Subarctic Pacific induces a large centric diatom bloom. Science 300, 958–961.

Turner, S.M., Nightingale, P.D., Spokes, L.J., Liddicoat, M.I., Liss, P.S., 1996. Increased dimethyl sulphide concentrations in sea water from in situ iron enrichment. Nature 383, 513–517.

Whitehead, R.F., de Mora, S.J., Demers, S., 2000. Enhanced UV radiation—a new problem for the marine environment. In: de Mora, S.J., Demers, S., Vernet, M. (Eds.), The Effects of UV Radiation in the Marine Environment. Cambridge University Press, Cambridge, UK, pp. 1–34.

Xie, H., Moore, R.M., Miller, W.L., 1998. Photochemical production of carbon disulphide in seawater. Journal Geophysical Research 103 (C3), 5635–5644.

Yocis, B.H., Kieber, D.J., Mopper, K., 2000. Photochemical production of hydrogen peroxide in Antarctic Waters. Deep-Sea Research I 47 (6), 1077–1099.

Zepp, R.G., Andreae, M.O., 1994. Factors affecting the photochemical production of carbonyl sulfide in seawater. Geophysical Research Letters 21 (25), 2813–2816.